EXPERIMENTS IN AN INITIAL REGION OF A CIRCULAR FREE JET

Yoshihiro Inoue*, Shintaro Yamashita* and Kunikazu Kondo**

* Dept. Mathematical & Design Eng., Gifu University, 1-1 Yanagido, Gifu 501-1193, Japan
E-mail: inouey@cc.gifu-u.ac.jp, yamasita@cc.gifu-u.ac.jp

** Dept. Mechanical Eng., Suzuka College of Tech., Shiroko-cho, Suzuka, Mie 510-0294, Japan
E-mail: kunikazu@mech.suzuka-ct.ac.jp

ABSTRACT

Coherent structures in the near field of an axisymmetric jet have been investigated in a water channel. Instantaneous velocity profiles were obtained in the axial and radial directions with the ultrasonic Doppler method. The UVP (ultrasonic velocity profile) monitor used in this study is Met-Flow model X3-PS with the ultrasonic transducers of the basic frequency of 4 MHz. Also, a multi-line measurement system was utilized. Two transducers were connected to the UVP monitor and alternately switched to acquire two profiles with different angles of azimuthal direction at the same streamwise position quasi-simultaneously. Dominant time-scale and averaged length-scale of velocity fluctuating fields are examined from DWT, and wavenumber-frequency spectrum is calculated by two-dimensional FFT along the axial direction. Coherent structures in the axial and radial directions are investigated in terms of POD. Axial variation in the amplitude and wavelength of $u(x, t)$ is well represented in the lower-order POD modes in the axial direction, and also the radial oscillation of the mixing layer is captured by the only first POD mode with about half a total energy. Azimuthal mode of radially oscillating mixing layer is estimated from a cross-correlation between the random coefficients $v^{(2)}(q, t)$ and $v^{(2)}(q + Dq, t)$.

Keywords : Round Jet, Discrete Wavelet Analysis, POD, Azimuthal Mode

INTRODUCTION

A study of the jet that is one of a representative flow field of free shear flow has been done a lot so far, and the engineering application field is wide. There are various kinds for a three-dimensional free jet from a difference of shape of an outlet. Of these, a circular jet [1], an elliptical jet [2], a rectangular jet [3] are well examined as a comparatively simple model.

This study is aimed for elucidation of space-time flow structure of a three-dimensional free jet by water tank experiment using an Ultrasonic Velocity Profile Monitor (UVP), putting a center of interest in the flow field close to the nozzle outlet. The authors have made experiments on a square and a circular jet and reported the fluctuating flow field of a square free-jet [4]. In this report, the flow structure of a circular free jet is examined.

A study of a circular jet is started for a long time, and Hinze describes the prospects of those days in the first edition of his book [5]. Interest for this flow field does not run out, and, for example, many experiments such as Wygnanski & Fiedller [1] are done afterwards. With experimental environment fixed better, experimental studies are still continued with progresses of experimental methods [6-8], and the understanding of flow structure is deepened; these studies contribute to high sophistication of a calculation model. In particular, the development of space measuring methods promotes a breakaway from conventional methods like point measurements, conditional measurements and so on, and it contributes greatly to understanding of the spatial structure of various flows.

The advantage of the ultrasonic Doppler method used in this study is to be able to get an instantaneous velocity profile on a line of ultrasonic beam in time series; the principle of the UVP measurements and its performance should be referred to Takeda [9]. On the other hand, a particle imaging velocimetry has ability to acquire two- or three-dimensional information in space, but it is not easy to expand this in the time direction. Therefore, the UVP measurements set in an appropriate measuring position and direction are very effective to obtain the information of space-time correlation of the flow field. In this study, acquired data are analyzed by Fourier transform, discrete wavelet transform and proper orthogonal decomposition, and, from their results, the flow structure of the circular jet is clarified.

EXPERIMENTAL PROCEDURE

Apparatus

The outline of flow field and coordinate system are shown in figure 1. We take x- and y-axes in the jet-axis and radial directions, respectively. Test section of the water tank used in this experiment is an open channel of 0.7 m wide, 0.64 m deep of water and 3 m long, and jet nozzle is set up at the central portion on the partition of the test section and settling chamber. The exit diameter of the nozzle is 85 mm, and the contraction shape is a quadrant of a radius 12 mm added hereafter a straight line. In the experiment, Reynolds number Re_j based on the velocity U_j in the core of the jet and nozzle exit diameter D was set to about 0.9×10^4. Then the initial momentum thickness q_0 of the shear layer at the position of $x / D = 0.2$ was about 1.0 mm, and $Re_\theta = U_j\, q_0 / n \approx 10^4$.

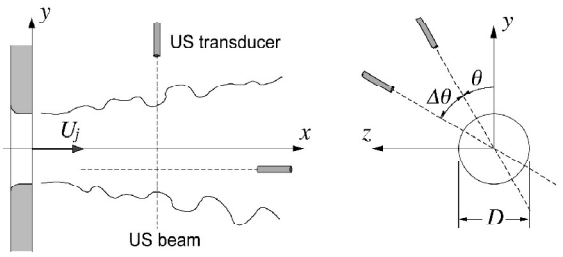

Fig. 1. Coordinate system

UVP measurement method

In the UVP measurement, ultrasonic transducer comprising a function of transmission and reception is used and velocity component in the traveling direction of ultrasonic beam is detected almost instantaneously for 128 points on the beam. The basic frequency of ultrasonic wave used in this experiment was 4 MHz, and hydrogen bubbles generated successively from a platinum wire of diameter of 30 μm was used for scattering particles. An incidence direction of the ultrasonic beam, namely, the measuring line was chosen as each direction of *x*- and *y*-axes as shown in figure 1, and the profiles along the *x*- and *y*-directions for the instantaneous velocity components of axial direction *u* and radial direction *v* were obtained in time series. In working conditions of this experiment, the time interval of velocity data was about 38 ms, and the space intervals of adjacent measuring point were 2.94 mm in the *x*-direction, and 2.20 mm in the *y*-direction.

In addition to the experiment using one transducer mentioned above, to examine the correlation of flow structure in the circumferential direction the experiment using two transducers simultaneously was also made. Azimuthal angle of the fixed measuring line is assumed *q*, and phase angle between the moving and fixed measuring lines is indicated by *Dq* (figure 1, right). In this case because multiplexer built in the UVP works, and sequential switching measurement is done, time delay of about 39 ms is occurred between the measuring lines in this measurement. The measuring position of the axial direction was $x / D =$ 2 and 3.

If a flight direction of ultrasonic beam is assumed *x*, the quantity obtained by this measurement is space-time distribution of *x* component of the instantaneous velocity, and it is expressed

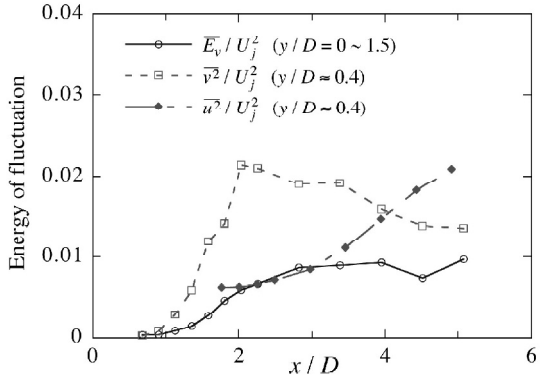

Fig. 3 Axial changes in the spatially and temporarily averaged energy of velocity fluctuation.

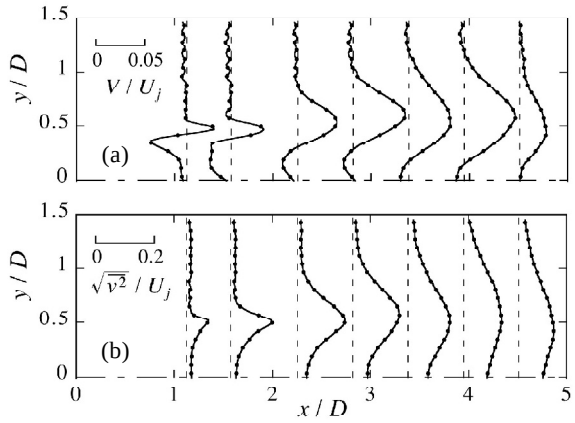

Fig. 2 Distributions of mean and fluctuating velocity components.

with $V_\xi(x) + v_\xi(x, t)$. Here $V_\xi(x)$ shows time-averaged velocity distribution and $v_\xi(x, t)$ space-time distribution of fluctuating velocity. For data set of this space-time distribution, data analyses such as Fourier transform, discrete wavelet transform and proper orthogonal decomposition are performed as done in the previous report [4], and flow structure is examined.

RESULTS AND DISCUSSION

Mean flow field

Figure 2 shows the distributions of radial component of mean velocity *V* and r.m.s. value of fluctuating velocity v_{rms} within the flow region in this experiment. Mean and fluctuating velocity profiles become anti-symmetric and symmetric, respectively, because of the axial symmetry of the flow. At $x / D = 1$, a sharp change of *V* around $y / D = 0.5$ is seen. This region is located between the jet core and the fluid surrounding jet, and is initial mixing layer that is comparatively thin. The mixing layer rapidly increases its thickness as goes downstream, and the fluctuation intensity in the layer is augmented. The fluctuation intensity has a distribution with its minimum at $y = 0$, and a difference of this local minimum and the peak value is shortened for $x / D > 4$.

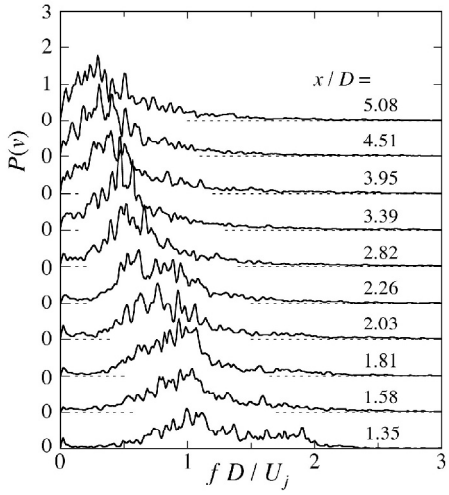

Fig. 4 Power spectrum of *v*-fluctuation at $y / D \approx 0.4$.

In order to inquire the axial change in the fluctuation energy, the changes in $\overline{u^2}$ and $\overline{v^2}$ at the representative position $y / D \approx 0.4$ and in space average of the energy of y component of fluctuating velocity $\overline{E_v}$ are shown in figure 3. Characteristic change is seen in $\overline{v^2}$ behavior in that it suddenly increases toward the maximum at $x / D = 2$, and thereafter it turns to decrease. Averaged fluctuating energy $\overline{E_v}$ increases in the range of $x / D < 3$, and becomes nearly constant afterwards. Unlike these, the distribution of $\overline{u^2}$ is monotone increasing in the measuring range. Figure 4 shows the power spectra of v-fluctuation. For $x / D < 2$, a high energy hump around the dimensionless frequency $f D / U_j = 1$ is seen, and this central frequency falls for $x / D > 2$. It seems that this change is caused by the distortion and/or coalescence behavior of the vortices formed in the mixing layer, and, as a result, the maximum of v-fluctuation energy at $x / D = 2$ is brought about.

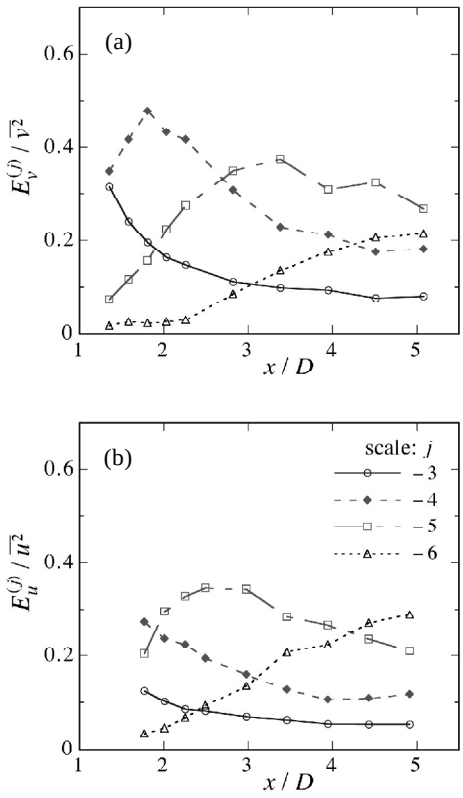

Fig. 5 Axial distributions of the wavelet spectrum of $v(t)$ and $u(t)$ at $y / D \approx 0.4$.

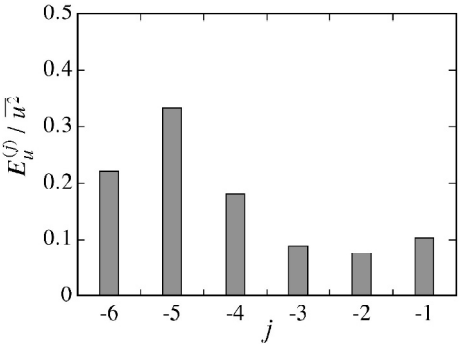

Fig. 6 Wavelet spectrum of $u(x, t)$ in space.

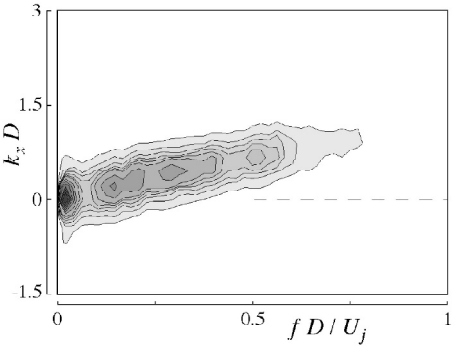

Fig. 7 Wavenumber-frequency spectrum of $u(x, t)$.

Consequently, to examine the axial change in the fluctuation energy included in each time scale, an orthogonal wavelet expansion for u- and v-fluctuations is made about time axis, and the change in the energy density of each scale is shown in figure 5. Because a time interval of this measurement is $Dt = 0.038$ s, for example, the time scale of the analysis for $j = -4$ becomes 0.61 s, and the dimensionless Nyquist frequency is 0.67. In figure 5(a) showing the change in v-fluctuation energy, the result shown in figure 4 becomes clearer, and the manner that a predominant scale in the axial direction varies can be grasped. That is, the fluctuation energies of $j = -3$ and -4 for $x / D < 2$, of $j = -4$ and -5 for $x / D = 2$ to 3.5 and of $j = -4$ to -6 for $x / D > 3.5$ are predominant. On the other hand, the change of a similar predominant scale is shown also in figure 5 (b) related to u-fluctuation energy, but energy contribution rate of scale $j = -4$ is small compared with v-fluctuation.

Mixing-layer oscillation in the axial direction

From $u(x, t)$ measured at $y / D = 0.4$, nearly central position in the mixing layer, the characteristic of the oscillation of the mixing layer in the axial direction is examined. At first figure 6

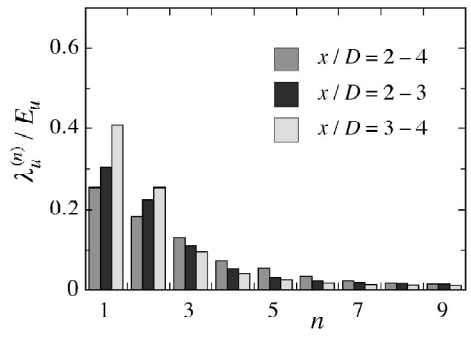

Fig. 8 POD spectrum of $u(x, t)$.

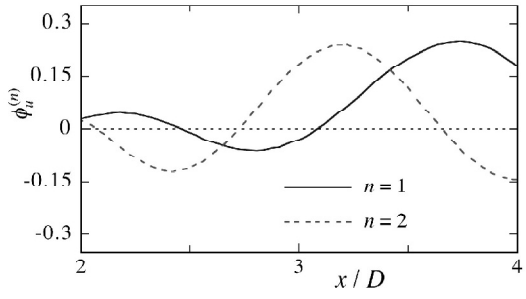

Fig. 9 Distributions of the eigenfunction at the first two POD modes in the axial direction at $y / D \approx 0.4$.

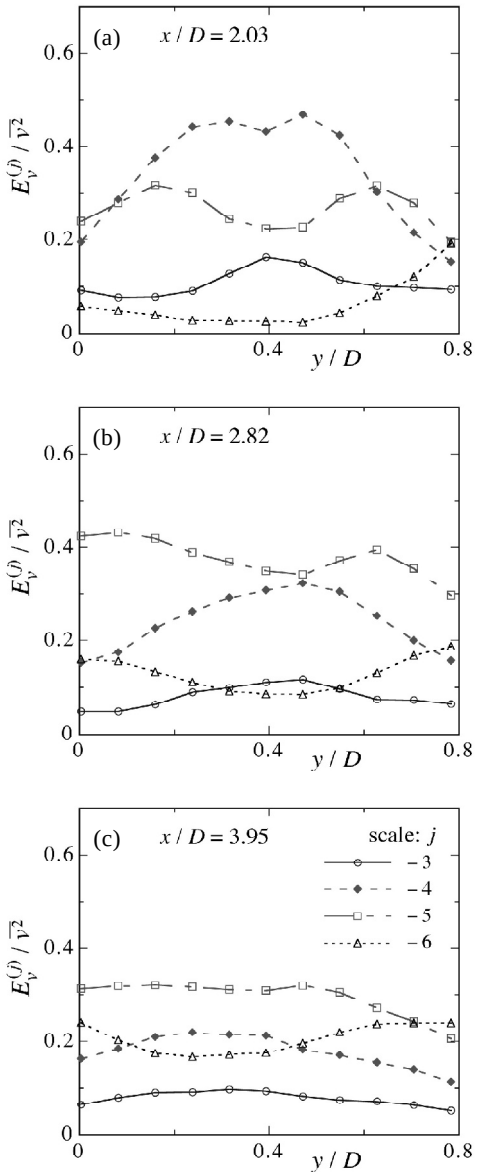

Fig. 10 Radial distributions of the wavelet spectrum of $v(y, t)$ in time. (a) $x / D = 2.03$, (b) $x / D = 2.82$ and (c) $x / D = 3.95$

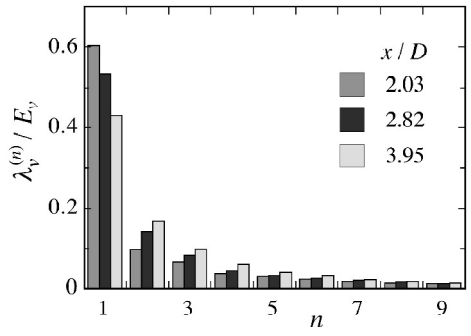

Fig. 11 POD spectrum of $v(y, t)$.

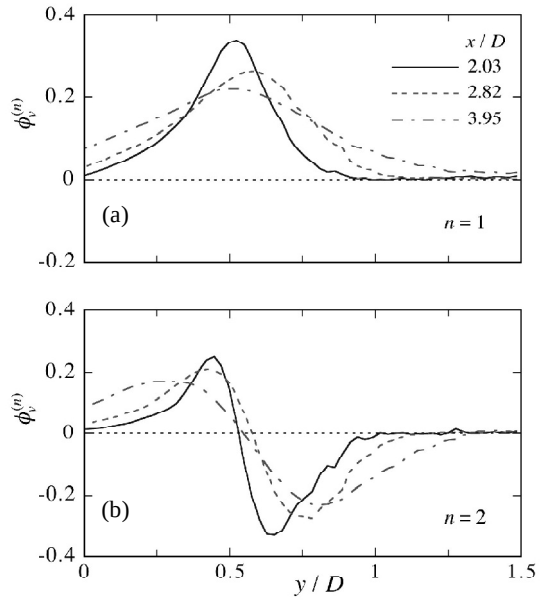

Fig. 12 Distributions of the eigenfunction at the first two POD modes.

is the DWT spectrum obtained from the orthogonal wavelet expansion made in the direction of spatial coordinate axis in the range of $x / D = 2$ to 5. From this figure, it can been seen that the energy contribution from the scale $j = -5$, which is the dimensionless wavelength 2.2, is the highest, and that there exist waves around the mean wavelength in the mixing layer.

Next, the wavenumber-frequency distribution is sought from two-dimensional Fourier transformation in spatiotemporal space. In this case the range of analysis was assumed $x / D = 3$ to 5. Figure 7 shows this result in the form of a contour map, where frequency f and wave number k_x are made dimensionless. The region where the energy is high extends as a ridge linearly from the origin, and the phase velocity of the wave is estimated 0.77 U_j for $y / D = 0.4$ from this slope.

As for this flow field, the time scale varies in the flow direction as described in the previous section, and it seems that the spatial scale varies with this. However, two-dimensional Fourier spectrum mentioned above cannot express non-homogeneity in space, and also DWT spectrum cannot. Therefore the proper orthogonal decomposition is performed for the same data set, and at first the spatial mode in which the energy content is high is detected. The result analyzed in the range of $x / D = 2$ to 4 is given in figure 9, and the energy spectrum is shown in figure 8. It is understood that, from the distribution of eigenfunction, the variations of the amplitude and wavelength in the flow direction are captured. Even if analyzed after dividing the target range into $x / D = 2$ to 3 and 3 to 4, any difference between the distributions of eigenfunction was hardly seen, but as shown in figure 8 the energy density of lower order mode is higher when analyzed after dividing, and in particular for $x / D = 3$ to 4.

Velocity fluctuation in the radial direction

The change of the time scale of v-fluctuation in the radial direction is examined using the DWT in representative positions $x / D = 2.03$, 2.82 and 3.95. It can been seen from figure 10 (a) of position $x / D = 2.03$ that the energy contribution from the scale $j = -4$ holds more than 40 % in the mixing layer, and that from $j = -5$ is large next. At $x / D = 2.82$ (figure 10 (b)) the contribution from the scale $j = -5$ is predominant on the whole. Because the scale $j = -5$ is the nearest to a column mode with respect to time scale, it seems that the column mode is dominant on the whole cross section of the jet at $x / D = 2.82$. On the other hand, the scales $j = -4$ and -5 make contribution of the same degree in the center of the mixing layer, and the fluctua-

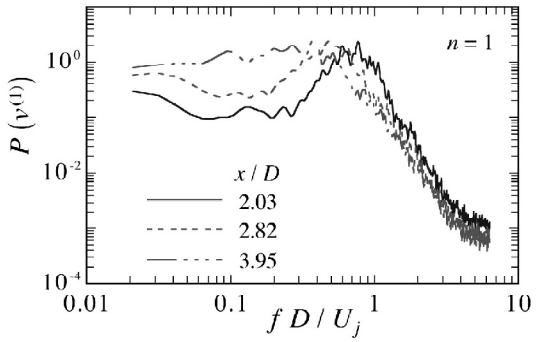

Fig. 13 Power spectra of the random coefficient at the first POD mode.

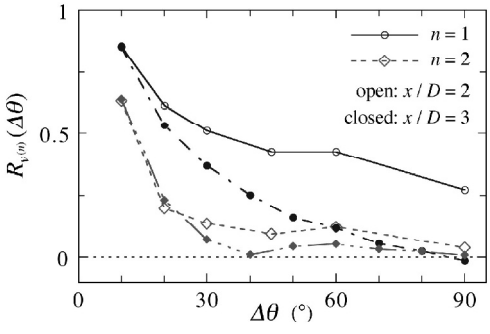

Fig. 14 Cross-correlation of the random coefficient of $v(y, t)$ in the azimuthal direction.

tion having a short time scale becomes stronger than in the jet center. The scale j = -5 is also predominant in x / D = 3.95 (figure 10 (c)), but its energy contribution becomes low, and the fluctuation of the scale j = -6 becomes relatively high compared with at the upstream positions.

For the radial distribution, the spatial mode was found by applying the proper orthogonal decomposition. Figure 11 gives the POD spectrum, and figure 12 shows the distributions of the eigenfunction for n = 1 and 2. The distributions of eigenfunction of low order mode in any position become similar, and only the radial width expands as goes downstream. From the energy spectra, extreme prominence of mode n = 1 is realized. However, this prominence becomes low in the downstream. It seems that the fluctuation of n = 1 corresponds to the inward and outward motions of the mixing layer from the distributions of the eigenfunction, and superposition of this fluctuation and that of n = 2 brings about a deviation of the radial position where v-fluctuation has a maximum value.

The power spectrum obtained from the FFT analysis of random coefficient $v^{(n)}(t)$ for n = 1 is shown in figure 13. From this spectrum, the time periodicity of the spatial variation of mode n = 1 can be examined. There exists a clear hill on the distributions of spectra for x / D = 2.03 and 2.82, and dimensionless frequency corresponding to each hill is about 0.8 and 0.5, respectively; these values accord with the peak frequencies seen in figure 4. On the other hand, the spectrum of x / D = 3.95 shifts more to the low-frequency side, but any hill with prominent frequency is not seen. Although the figure was omitted by limitation of the space, any prominent component in the spectra for n = 2 does not appear in all positions, and hence there seems to be little relevance between the generation of spatial fluctuation for n = 2 and the mechanism to produce the fluctuation for n = 1.

Velocity correlation in the azimuthal direction

The experiment on the flow structure in the circumference direction was made on the two measuring lines which are aligned to the radial direction and different in phase angle; the phase angle Dq was varied from 10° to 90°. As was also described in the previous section, the motion in the jet cross section can be well expressed by the lower-order POD mode of $v(y, t)$, and this time fluctuation can be contracted to the random coefficient $v^{(n)}(t)$. On the confirmation that the eigenvalue and eigenfunction do not change in the circumferential direction, we understand that the circumferential change affects only the random coefficient; we put this as $v^{(n)}(q, t)$. Here, a characteristic between the random coefficients with different phase angles is examined from cross correlation.

Figures 14 (a) and (b) stand for the circumferential cross-correlation coefficients of $v^{(1)}$ and $v^{(2)}$ at x / D = 2 and 3 respectively. Values of correlation coefficient of $v^{(1)}$ decrease with increase of Dq at all positions, and those for x / D = 2 maintain the value of 0.3 to 0.5 at Dq = 90° whereas for x / D = 3 there is almost no correlation at the same phase angle. This means high axially-symmetric nature of the fluctuation at x / D = 2, and the decrease in correlation length namely the poorness of axial symmetry is exhibited at the downstream position. In addition, values of correlation coefficient of $v^{(2)}$ for x / D = 2 suddenly decrease to approximately 0 from Dq = 0° to 40°, and correlation length in the circumferential direction is considerably short. If this spatial mode means the oscillation of the center of the mixing layer in the radial direction as mentioned in the above section, this flow has structures of scale of 60° to 80° in circumferential span, and it seems that five or six structures are arranged in the whole circumference. This result agrees well with the result of flow visualization made particularly as well as the experimental result of Toyoda [10].

CONCLUSIONS

Results of this study are summarized below.

(1) The energy of fluctuating velocity in the mixing layer began to rapidly increase from $x / D \approx 1$, and v-fluctuation grew up firstly. The time scale of fluctuation shifted to the lower frequency side in the process of this growth, and the difference of u- and v-fluctuations appeared in DWT scale j = -4, which is the dimensionless Nyquist frequency of 0.67.

(2) Mean wavelength of the fluctuation and phase velocity were estimated from axial velocity distribution at $y / D \approx 0.4$. In addition, the change of the wavelength in the flow direction was well expressed by the distribution of eigenfunction found with POD.

(3) Nearly 50 % of total energy of the fluctuation were contained only in the first mode of POD for $v(y, t)$, and this time scale was about 0.8 and 0.5 in dimensionless frequency at x / D = 2.03 and 2.82, respectively.

(4) It was shown that the axial symmetry became poor in the axial direction from the measurement of phase of $v(y, t)$ along the circumferential direction, and the scale of the flow structure in the circumferential span was estimated as 60° to 80° from the fluctuating component of the second mode of POD.

REFERENCES

1. I. Wygnanski, I., H. Fiedler, 1969, Some measurements in the self-preserving jet, *J. Fluid Mech.*, 38, pp. 577-612.
2. H.S. Husain, F. Hussain, 1993, Elliptic jets. Part 3. Dynamics of preferred mode coherent structure, *J. Fluid Mech.*, 248, pp. 315-361.
3. Y. Tsuchiya, C. Horikoshi, T. Sato, 1986, On the spread of rectangular jets, *Exp. Fluids*, 4, pp. 197-204.
4. Y. Inoue, S. Yamashita, K. Kondo, 2002, The ultrasonic velocity profile measurement of flow structure in the near field of a square free jet, *Exp. Fluids*, 32, pp. 170-178.
5. J.O. Hinze, 1959, "Turbulence. An Introduction to Its Mechanism and Theory," McGraw-Hill, New York.
6. N.R. Panchapakesan, J.L. Lumley, 1993, Turbulence measurements in axisymmetric jets of air and helium. Part 1. Air jet, *J. Fluid Mech.*, 246, pp. 197-223.
7. H.J. Hussein, S.P. Capp, W.K. George, 1994, Velocity measurements in a high-Reynolds-number, momentum-conserving, axisymmetric, turbulent jet, *J. Fluid Mech.*, 258, pp. 31-75.
8. G. Xu, R.A. Antonia, 2002, Effect of different initial conditions on a turbulent round free jet, *Exp. Fluids*, 33, pp. 677-683.
9. Y. Takeda, 1995, Velocity profile measurement by ultrasonic Doppler method, *Exp. Thermal Fluid Sci.*, 10, pp. 444-453.
10. K. Toyoda et al., 1999, Effect of axial azimuthal perturbations on entrainment, mixing and diffusion of a circular jet, *Proc. 3rd ASME/JSME Joint Fluids Eng. Conf.*, FEDSM99-7285.